Biochimica et Biophysica Acta 1850 (2015) 88–96

Contents lists available at ScienceDirect

Biochimica et Biophysica Acta

journal homepage: www.elsevier.com/locate/bbagen

The UDP-glucose pyrophosphorylase from *Giardia lamblia* is redox regulated and exhibits promiscuity to use galactose-1-phosphate

Ana C. Ebrecht [1], Matías D. Asención Diez [1], Claudia V. Piattoni, Sergio A. Guerrero, Alberto A. Iglesias *

Instituto de Agrobiotecnología del Litoral (UNL-CONICET), Facultad de Bioquímica y Ciencias Biológicas, Ciudad Universitaria, Paraje "El Pozo" CC 242, S3000ZAA Santa Fe, Argentina

ARTICLE INFO

Article history:
Received 19 March 2014
Received in revised form 26 August 2014
Accepted 6 October 2014
Available online 12 October 2014

Keywords:
UDP-glucose pyrophosphorylase
Redox regulated
Glucose-1-phosphate
Galactose-1-phosphate
Carbohydrate metabolism

ABSTRACT

Background: Giardia lamblia is a pathogen of humans and other vertebrates. The synthesis of glycogen and of structural oligo and polysaccharides critically determine the parasite's capacity for survival and pathogenicity. These characteristics establish that UDP-glucose is a relevant metabolite, as it is a main substrate to initiate varied carbohydrate metabolic routes.
Results: Herein, we report the molecular cloning of the gene encoding UDP-glucose pyrophosphorylase from genomic DNA of *G. lamblia*, followed by its heterologous expression in *Escherichia coli*. The purified recombinant enzyme was characterized to have a monomeric structure. Glucose-1-phosphate and UTP were preferred substrates, but the enzyme also used galactose-1-phosphate and TTP. The catalytic efficiency to synthesize UDP-galactose was significant. Oxidation by physiological compounds (hydrogen peroxide and nitric oxide) inactivated the enzyme and the process was reverted after reduction by cysteine and thioredoxin. UDP-N-acetyl-glucosamine pyrophosphorylase, the other UTP-related enzyme in the parasite, neither used galactose-1-phosphate nor was affected by redox modification.
Conclusions: Our results suggest that in *G. lamblia* the UDP-glucose pyrophosphorylase is regulated by oxido-reduction mechanism. The enzyme exhibits the ability to synthesize UDP-glucose and UDP-galactose and it plays a key role providing substrates to glycosyl transferases that produce oligo and polysaccharides.
General significance: The characterization of the *G. lamblia* UDP-glucose pyrophosphorylase reinforces the view that in protozoa this enzyme is regulated by a redox mechanism. As well, we propose a new pathway for UDP-galactose production mediated by the promiscuous UDP-glucose pyrophosphorylase of this organism.

1. Introduction

UDP-glucose (UDP-Glc) is a key intermediate for carbohydrate metabolism, mainly for the synthesis of oligo and polysaccharides in different organisms [1]. UDP-Glc pyrophosphorylase (EC 2.7.7.29; UDP-Glc PPase) catalyzes the production of the sugar-nucleotide (in presence of Mg^{2+}) according to the reaction: Glc-1P + UTP ⟷ UDP-Glc + PPi. Although it is ubiquitously distributed in nature (including animals, plants and microorganisms) [1–3], the enzyme from eukaryotes is remarkably unrelated with that found in prokaryotes and they are not homologous proteins [2,4,5]. Recently [6], it has been demonstrated that the UDP-Glc PPase from *Entamoeba histolytica* is finely regulated by post-translational redox modification elicited by critical metabolites of the intracellular environment. The regulation is determinant for the distribution of carbohydrates into different metabolic fates. This former work opened the question if the kinetic and regulatory behavior of the *E. histolytica* enzyme is common between UDP-Glc PPases from protozoa.

Giardia lamblia is a flagellated protozoan having a limited metabolic repertoire in comparison with common parasites and exhibiting adaptation to microaerophilic environments [7,8]. It is the causative agent of giardiasis, an intestinal dysenteric disease distributed worldwide and affecting humans and other vertebrates. The parasite life cycle is represented by the trophozoites that colonize the small intestines and the infectious cysts, which are eliminated in the faeces to the environment. The protective cystic wall comprises a characteristic N-acetyl-galactosamine polysaccharide and the structure is responsible for the parasite survival outside the host [9,10]. Furthermore, *G. lamblia* accumulates glycogen, which serves as an energy reserve in trophozoites [11] and also plays a critical role in their differentiation to cyst forms [12].

Despite the relevance of polysaccharides for survival and pathogenicity of the parasite, the complete characterization of the enzymes involved in carbohydrates metabolism in *Giardia* is far from complete. The pathway for cyst wall synthesis has been the more studied and the kinetic properties of the UDP-*N*-acetyl-glucosamine pyrophosphorylase from *G. lamblia* (*Gla*UDP-GlcNAc PPase) were determined with some detail, either for the enzyme purified from the source [13]

* Corresponding author at: Laboratorio de Enzimología Molecular, IAL–FBCB Paraje "El Pozo" CC 242, S3000ZAA Santa Fe, Argentina. Tel./fax: +54 342 4575209x217.
E-mail address: iglesias@fbcb.unl.edu.ar (A.A. Iglesias).
[1] Both authors contributed equally to the work.

http://dx.doi.org/10.1016/j.bbagen.2014.10.002
0304-4165/

or produced recombinantly [14,15]. Conversely, no report is available concerning generation of UDP-Glc, the glycosyl donor for glycogen elongation in this protozoan [16,17]. Herein, we present the molecular cloning, heterologous expression, and purification the UDP-Glc pyrophosphorylase from *G. lamblia* (*Gla*UDP-Glc PPase). We performed the kinetic characterization of the recombinant enzyme, which exhibited promiscuity for using Gal-1P (besides its major activity with Glc-1P) and sensitivity to modification by redox agents. The properties of *Gla*UDP-Glc PPase are analyzed in comparison with those reported for the homologous enzyme from other protozoa as well as for *Gla*UDP-GlcNAc PPase. The results are discussed in relation with the metabolic scenario for polysaccharides taking place in the microorganism.

2. Materials and methods

2.1. Chemicals

Glc-1P, Gal-1P, GlcN-1P, GalN-1P, GlcNAc-1P, UTP, TTP, H_2O_2, diamide, DTT, L-cysteine (Cys), L-cystine (CySS), sodium nitroprusside (SNP), protein standards, antibiotics, isopropyl-β-thiogalactoside (IPTG) and oligonucleotides were obtained from Sigma-Aldrich (St. Louis, MO, USA). All other reagents were of the highest quality available.

2.2. Bacteria and plasmids

Escherichia coli Top 10 F′ (Invitrogen, Carlsbad, CA, USA) cells and pGEM®T Easy (Promega, Fitchburg, WI, USA) vector were used for cloning purposes. Genes were expressed using pET19b (Novagen, Madison, WI, USA) and pRSETA (Invitrogen) vectors and *E. coli* BL21 (DE3) (Invitrogen) as host. DNA manipulations and *E. coli* cultures as well as transformations were performed according to standard protocols [18].

2.3. Amplification and cloning of ugp and uap genes from G. lamblia

The genes *ugp* (Gene ID: 5699477) and *uap* (Gene ID: 5700112) coding for *Gla*UDP-Glc and *Gla*UDP-GlcNAc PPases, respectively, were amplified by PCR from genomic *G. lamblia* WB-assemblage A DNA kindly provided by Dr. Hugo Lujan (Universidad Católica de Córdoba-CONICET, Argentina). Specific sense primers, containing *Nde*I or *Bam*HI sites, and antisense primers, containing *Eco*RI site, were designed for subcloning both enzymes. Primers for *Gla*UDP-Glc PPase were: *ugp*Fow (5′-CATATGTCCTATCAGGATCTGCTCAGCGC-3′) and *ugp*Rev (5′-GAATTCTCACTGTCCCAGAGTGCAAT-3′); whereas primers for *Gla*UDP-GlcNAc PPase were: (5′-GGATCCATGCCAGGCCTGGAGGAGTTTCTT-3′) and *UAP*Rev (5′-GAATTCCTAGACGGCCTTCACGCTAGA-3′). Restriction sites are underlined.

All PCR reaction mixtures (50 μL) contained 100 ng of genomic DNA, 2 pg of each primer; 0.2 mM of each dNTP; 1.5 mM Mg^{2+} and 1 U *Taq* DNA polymerase (Fermentas, St. Leon-Rot, Germany). Standard conditions of PCR were used for 30 cycles: denaturing at 94 °C for 1 min; annealing at 50 °C for 1 min and extension at 72 °C for 2 min, with a final extension of 10 min at 72 °C. PCR reaction mixtures were electrophoretically defined in 1% (*w*/*v*) agarose gel and purified with Wizard SV gel & PCR Clean Up system (Promega), according to the manufacturer's instructions. Amplified genes were cloned into the T-tailed plasmid pGEM-TEasy and identities were confirmed by DNA sequencing (MacroGen, Seoul, Korea). The *ugp* gene was sub-cloned into pET19b *Nde*I/*Eco*RI sites and *uap* into pRSETA *Bam*HI/*Eco*RI sites, to obtain pUGP and pUAP expressing plasmids, respectively. These constructs were used to transform *E. coli* BL21 (DE3) competent cells. By means of these cloning strategies, both enzymes were produced with an N-terminal His-tag to facilitate purification procedures.

2.4. Protein expression and purification

Cells of *E. coli* BL21 (DE3) transformed with either pUGP or pUAP were grown at 37 °C in LB medium supplemented with 100 μg/ml ampicillin until reach an OD_{600} ~ 0.6. Protein expression was induced with 0.4 mM IPTG at 25 °C for 20 h. Cells were harvested by centrifuging 15 min at 4 °C and 5000 ×*g*, and the pellet was resuspended in 5 ml of *buffer A* (25 mM Tris–HCl pH 8.0, 300 mM NaCl, 5% (v/v) glycerol, 10 mM imidazole) per g of cells. Cells were disrupted by sonication on ice, eight pulses for 30 s with 60 s intervals and centrifugation at 16,000 rpm for 20 min at 4 °C.

Both *Gla*UDP-Glc PPase and *Gla*UDP-GlcNAc PPase were purified by ion metal affinity chromatography (IMAC), using 1 ml HisTrap™ HP columns (GE Healthcare, Piscataway, NJ, USA). Briefly, supernatants were loaded onto previously equilibrated Ni^{2+}-charged columns. After extensively washing with *buffer A*, samples were eluted with a 10–300 mM imidazole lineal gradient (50 column volumes). Active fractions were pooled, dialyzed to remove imidazole and supplemented with 10% (v/v) glycerol, 2 mM DTT and 0.1 mM EDTA. All proteins were stable for at least six months when stored at −80 °C under these conditions.

2.5. Protein methods

Protein concentration was determined by the Bradford procedure [19] using bovine serum albumin as a standard. Recombinant proteins were defined electrophoretically in sodium dodecyl sulphate polyacrylamide gels (SDS-PAGE) according to Laemmli [20] to check for purity. Gels were stained with Coomassie Brilliant Blue.

2.6. Molecular mass determination

To determine the native structure of *Gla*UDP-Glc PPase and *Gla*UDP-GlcNAc PPase, purified enzymes were subjected to gel filtration chromatography. Samples were loaded in a Superdex Tricorn 5/200 column (GE Healthcare) in *buffer B* (50 mM HEPES–NaOH pH 8.0, 100 mM NaCl, and 0.1 mM EDTA). The molecular mass was calculated using a calibration plot constructed with protein standards from GE Healthcare, including thyroglobulin (669 kDa), ferritin (440 kDa), aldolase (158 kDa), conalbumin (75 kDa), and ovalbumin (44 kDa). The column void volume was measured using a dextran blue loading solution (Promega). To determine the effect of oxidation in the native structure of *Gla*UDP-Glc PPase, the enzyme was incubated 40 min (25 °C) with either 5 mM DTT or 2 mM H_2O_2. After treatment the samples were analyzed by gel filtration.

2.7. Enzyme assay

*Gla*UDP-Glc PPase activity was assayed in the UDP-Glc synthesis way measuring inorganic phosphate (P_i) released after hydrolysis of pyrophosphate (PP_i) by using the highly sensitive colorimetric method described elsewhere [21]. Standard reaction mixtures contained 100 mM MOPS-HCl (pH 8.0), 10 mM $MgCl_2$, 1 mM UTP, 2 mM DTT, 0.2 mg/ml bovine serum albumin, 0.5 mU/μl yeast inorganic pyrophosphatase and a proper enzyme dilution. Assays were initiated by addition of 1 mM Glc-1P in a total volume of 50 μl. Reaction mixtures were incubated for 10 min at 37 °C and terminated by adding the Malachite Green reactive. The complex formed with the released P_i was measured at 630 nm with an ELISA EMax detector (Molecular Devices). Controls were made to ensure the measurement of initial velocity (v_o), that is the rate where product formation was practically linear with time and the total consumption of substrates was below 10% [22,23]. As shown in Fig. S1, at 10 min of reaction it was assured linearity in the formation of product with time for measurements of activity of *Gla*UDP-Glc PPase and GlaUDP-GlcNAc PPase under the different conditions of substrates concentrations. One unit (U) of enzyme activity is equal to 1 μmol of

product formed per minute under the respective assay conditions specified above. For measurements of *Gla*UDP-GlcNAc PPase activity reactions were conducted exactly as before and started with 1 mM GlcNAc-1P. As well, the same procedure was followed for the analysis of enzyme promiscuity towards sugar-1P, except that in this case, the different monosaccharide-1Ps were included in the assay mixture and reactions were started with UTP.

2.8. Calculation of kinetic constants

Kinetic assays were performed using specified concentrations and conditions for all reaction mixture components. For the kinetic studies enzyme was fully reduced by maintenance, in the presence of 2 mM DTT and checked for full activity. Saturation curves were performed by assaying the respective enzyme activity at saturating level of a fixed substrate and different concentrations of the variable substrate. The experimental data were plotted as enzyme activity (U/mg) versus substrate concentration (mM), and kinetic constants were determined by fitting the data to the modified Hill equation: $v_o = V_{max}\,[S]^n/(S_{0.5}{}^n + [S]^n)$, as described elsewhere [24], using the Levenberg–Marquardt nonlinear least-squares algorithm provided by the computer program Origin™ 8.0. Hill plots were used to calculate the Hill coefficient (n), measuring the interaction degree (cooperativity) between kinetically different binding sites per mole of enzyme [25,26]; the maximal velocity (V_{max}); and the kinetic constants that correspond to the substrate concentrations giving 50% of the maximal velocity ($S_{0.5}$). All kinetic constants are the mean of at least three sets of data, which were reproducible within ±10%.

2.9. Oxidation assay

Purified *Gla*UDP-Glc PPase and *Gla*UDP-GlcNAc PPase were desalted using Microcon spin columns (Millipore) to *buffer C* (100 mM MOPS-HCl pH 8.0, 0.1 mM EDTA) to remove DTT. For oxidation, 0.5 μM of each enzyme was incubated in *buffer C* at 25 °C with different concentrations of either diamide, H_2O_2 or SNP. Incubations with SNP were conducted in presence of a direct environment light to induce reagent's photolytic decomposition and generate nitric oxide and other reactive nitrogen species [27]. After different incubation times, aliquots were withdrawn, diluted and assayed for activity as above described.

Experimental data were plotted as log remaining activity versus oxidation time (min). For calculation of percentage of remaining activity, 100% was considered as the activity when the enzyme was incubated under the same conditions but in the absence of oxidants. Oxidation kinetics was analyzed as described elsewhere [6,28]. Briefly, the first order rate constant (k_{app}) for each oxidant concentration was calculated by fitting the curves to the equation: log relative activity $= 2 - k_{app} * t$, using Origin™ 8.0 software. Plots of k_{app} values versus variable oxidant concentrations allowed k_i (maximum rate of inactivation achieved at an infinite concentration of inactivator), K_i (inhibitor concentration yielding a rate of inactivation equal to half of the k_i), and k'' ($k'' = k_i/K_i$, the second-order rate, which is considered to be the best measure of relative inactivator potency) determination. Experimental points determined in redox modification studies are means of at least three measurements reproducible within ±10%.

2.10. Reduction assay

To remove any oxidant excess, the oxidized enzymes (as specified above) were diluted and extensively desalted/re-concentrated to 0.5 μM in 50 mM MOPS-HCl pH 8.0 by means of Microcon spin columns (Millipore). The oxidized enzymes were incubated with different reducing agents: 2.5 mM DTT, 5 mM L-Cys, 50 μM *Trypanosoma cruzi* TRX (*Tcr*TRX) or 50 μM *T. cruzi* tryparedoxin (*Tcr*TXN) in buffer 50 mM MOPS-HCl pH 8.0. After 30 min incubation, aliquots were withdrawn from the incubation media and assayed for enzyme activity. Before use, *Tcr*TRX and *Tcr*TXN were reduced by incubation in buffer 100 mM MOPS-HCl pH 8.0, 5% (*v*/*v*) glycerol, 0.1 mM EDTA, and 0.5 mM DTT during 30 min at 25 °C. Thiol proteins used for assays were purified according to protocols previously specified [6,29].

2.11. Enzyme behavior at different redox potential

The medium reduction potential (E_m) of a protein is defined as the reduction potential in which the concentrations of its oxidized and reduced forms are equal [30]. The E_m of *Gla*UDP-Glc PPase and *Gla*UDP-GlcNAc PPase were determined by redox titration with Cys/CySS, the reduced and oxidized species of L-cysteine, respectively. Different reduction potential values (E_h) were obtained varying the relative concentrations of both species, maintaining the total concentration fixed at 1 mM, with the addition of 100 mM MOPS-HCl pH 7.4. Values of E_h were calculated by using the Nernst equation: $E_h = E_o - RT/nF\ ln\ [Cys]^2/[CySS]$, where E_o is the E_h for Cys/CySS at pH 7.4 (−0.250 V) [31], R is the universal gas constant (8.314 J K^{-1} mol^{-1}), T is the absolute temperature (298 K), n is the number of moles of electrons transferred in the reaction (2), F is the Faraday constant (96,485 J mol^{-1} V^{-1}), and $[Cys]^2/[CySS]$ is the ratio between the concentrations of both redox species [32].

*Gla*UDP-Glc PPase and *Gla*UDP-GlcNAc PPase were incubated in a final concentration of 0.5 μM during 2 h at room temperature in different redox buffers (to reach redox equilibrium). Aliquots of treated samples were taken and enzyme activity was assayed for both enzymes under standard conditions (see above). Data were plotted as percentage of activity versus E_h, where the highest activity for each enzyme was set as 100% of activity.

3. Results

3.1. Cloning and heterologous expression of G. lamblia genes encoding UDP-Glc PPase and UDP-GlcNAc PPase

It has been reported that *G. lamblia* accumulates glycogen for storage of carbon and energy [11,12]. To get a better picture of occurrence and synthesis of the reserve polysaccharide in *G. lamblia* we approached the study of UDP-Glc PPase, the enzyme that catalyzes synthesis of the glycosyl donor (UDP-Glc) for glycogen elongation in heterotrophic eukaryotes [16,17]. Thus, *G. lamblia* ATCC50803 genome analysis showed two genes linked to UTP-dependent pyrophosphorylases [8,33]: one nucleotide sequence encoding a putative UDP-Glc PPase (*ugp*, Gene ID: 5699477) and another gene coding for UDP-GlcNAc PPase (*uap*, Gene ID: 5700112). The latter enzyme has already been studied in detail [13,15,34]. The *ugp* gene sequence predicts a 450 amino acid protein (*Gla*UDP-Glc PPase) with a theoretical 49.3 kDa molecular mass, which shares ~30% identity with UDP-Glc PPases from other protozoa: *E. histolytica* (*Ehi*UDP-Glc PPase) [6], *Trypanosoma brucei* [35] and *Leishmania major* [36]. In addition, the predicted *Gla*UDP-Glc PPase has a similar identity degree with the homologous enzyme from other non-protozoa eukaryotes: *Saccharomyces cerevisiae* (33.3%) [37] and bovine liver (35.5%) [38]. Curiously, a higher identity (slightly above 40%) is found between the UDP-Glc PPases from *G. lamblia* and barley [39]. On the other hand, *uap* encodes for a protein of 436 amino acids, with a molecular mass of 48.3 kDa, according to previous reports dealing with characterization of the UDP-GlcNAc PPase from *G. lamblia* [13,15,34].

We designed specific primers to amplify the genes *ugp* (1353 bp lenght) and *uap* (1310 bp) from *G. lamblia* genomic DNA in single-step PCR procedures. After confirming the identity by sequencing DNA the amplified products were used to construct the pUGP and pUAP vectors (see Materials and methods section), express them into *E. coli* BL21 (DE3) cells and produce *Gla*UDP-Glc PPase and *Gla*UDP-GlcNAc PPase, respectively. Both recombinant proteins were over-expressed in the soluble fractions (Fig. 1, lanes 2 and 4), and they were purified to a high degree using a single step of IMAC (Ni^{2+}), as judged by the

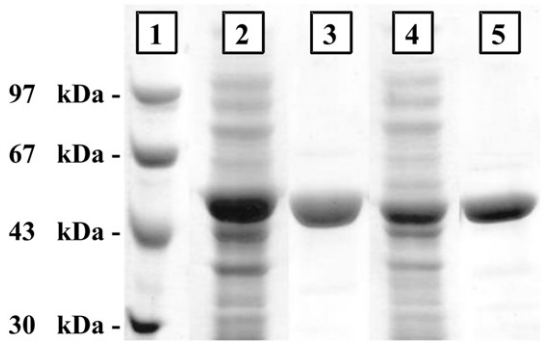

Fig. 1. SDS-PAGE of recombinant *Gla*UDP-Glc PPase and *Gla*UDP-GlcNAc PPase. Lane 1: Molecular mass markers; Lane 2: *Gla*UDP-Glc PPase over-expression in crude extracts; Lane 3: Purified *Gla*UDP-Glc PPase; Lane 4: *Gla*UDP-GlcNAc PPase over-expression in crude extracts; Lane 5: Purified *Gla*UDP-GlcNAc PPase. Purifications were conducted as described under the Materials and methods section.

SDS-PAGE analysis (Fig. 1, lanes 3 and 5). In experiments of gel filtration chromatography on Superdex 200 the *Gla*UDP-Glc PPase eluted as a single peak corresponding to a 50 kDa molecular mass. No higher oligomeric conformations were observed, thus suggesting stability of the monomeric form; according to previous reports for the enzyme from *E. hystolitica* [6] and *L. major* [36]. *Gla*UDP-GlcNAc PPase also eluted in a single peak with an estimated molecular mass of 50 kDa, which is in good agreement with that found in previous studies [15].

3.2. Kinetic characterization and substrate specificity analysis of G. lamblia UDP-Glc PPase

Since in non-photosynthetic eukaryotic organisms glycogen synthesis occurs via UDP-Glc, the study of the kinetic properties of *Gla*UDP-Glc PPase arises as relevant to understand metabolism of carbohydrates in the protozoan. As expected, the enzyme exhibited a strict dependence on Mg^{2+} to catalyze the synthesis of UDP-Glc and PP_i from UTP and Glc-1P, with the kinetic parameters that are summarized in Table 1. The V_{max} determined for the enzyme is comparable to that reported for UDP-Glc PPases from other eukaryotic sources that also exhibit high specific activity [37,40,41]. Saturation plots for both substrates adjusted near to a hyperbolic behavior, with $S_{0.5}$ values ~0.15 mM (Table 1); which are similar to what has been reported for the enzyme from other eukaryotes [35,36,41]. However, *Gla*UDP-Glc PPase has a lower $S_{0.5}$ value for substrates when compared with homolog enzymes from potato tuber [40], *E. histolytica* (this also showing a lower V_{max}) [6], and the extensively characterized UDP-Glc PPase from barley [42].

To further study the *Gla*UDP-Glc PPase kinetic properties we explored the ability of the enzyme to use alternative substrates to synthesize different nucleotide-sugars. Concerning nucleotides, the enzyme was able to utilize TTP, but not ATP, GTP, nor CTP (tested up to 2.0 mM). Enzyme kinetics for TDP-Glc synthesis showed lower value of V_{max} (30-fold) as well as a higher $S_{0.5}$ for substrates (6-fold for TTP and 3-fold for Glc-1P); with a slight increase in the n value for both substrates when compared with the production of UDP-Glc (see Table 1). Then, the catalytic efficiency (defined as $V_{max}/(S_{0.5})^n$, analogous to V_{max}/K_m for hyperbolic kinetics [25]) of *Gla*UDP-Glc PPase for using UTP was about two orders of magnitude higher than for TTP.

In a same way, we analyzed specificity of *Gla*UDP-Glc PPase towards Glc-1P by testing as alternative substrates Man-1P, Fru-1P, Gal-1P, GlcNAc-1P, GlcN-1P or GalN-1P (each one added at 2 mM into the assay mixture). The enzyme exhibited a poor activity (less than 1%) using these sugar-1Ps, except for Gal-1P. Indeed, the activity measured with 2 mM Gal-1P was ~30% of that determined with Glc-1P. Afterwards, saturation kinetics for Gal-1P were performed and analyzed in comparison with Glc-1P, using 1 mM UTP. As shown in Fig. 2, *Gla*UDP-Glc PPase exhibited a similar apparent affinity for using both hexose-1Ps; although the V_{max} determined with Gal-1P was lower and the n increased when compared to Glc-1P (Table 1). Thus, the catalytic efficiency for the alternative substrate Gal-1P is similar when compared with Glc-1P, whilst it is ~3-fold higher for UTP when the nucleotide is utilized in combination with Gal-1P instead of Glc-1P. After these results, we analyzed for the possible use of different sugar-1Ps (as alternative substrate to Glc-1P) by the recently characterized *Ehi*UDP-Glc PPase [6]; but in our hands the entamoebic enzyme showed negligible activity with any of the alternative substrates, including Gal-1P. A similar behavior was observed for *Gla*UDP-GlcNAc PPase, which resulted highly specific for GlcNAc-1P, in agreement with previous reports [15].

Table 1
Kinetic parameters for *Gla*UDP-Glc PPase. Parameters were calculated from average data from three independent experiments, as detailed under the Materials and methods section.

Synthesis of	Substrate	$S_{0.5}$ (mM)	n	V_{max} (U/mg)	$V_{max}/(S_{0.5})^n$ (U/mg mM)
UDP-Glc	Glc-1P	0.13 ± 0.01	1.1	400 ± 21	3773
	UTP	0.14 ± 0.02	1.1		3478
TDP-Glc	Glc-1P	0.36 ± 0.04	1.2	14 ± 2	47
	TTP	0.90 ± 0.02	1.5		16
UDP-Gal	Gal-1P	0.09 ± 0.01	1.5	75 ± 8	2778
	UTP	0.08 ± 0.01	1.9		9103

3.3. Redox modification of GlaUDP-Glc PPase and GlaUDP-GlcNAc PPase

Recently, it was demonstrated that the *Ehi*UDP-Glc PPase is regulated by a redox mechanisms [6]. The enzyme is reversibly inactivated by oxidation with reactive oxygen and nitrogen species (ROS and RNS, respectively) and the activity is restored by the action of reducing agents. It is known that amino acids containing sulfur are modified by redox mechanisms and are consequently involved in modulation of the enzyme activity. Supplemental Fig. 2 depicts an amino acids alignment between the entamoebic enzyme and the two pyrophosphorylases from *G. lamblia*, allowing the identification of critical residues responsible for redox modification. *Ehi*UDP-Glc PPase contains five cysteine and eleven methionine residues but it was shown that only Cys^{108}, Cys^{378} and Met^{106} are critical for redox modulation of the enzyme activity. In comparison, *Gla*UDP-Glc PPase (sharing 33% identity with the entamoebic homolog) contains fourteen cysteine and nine methionine residues. Fig. 3 shows critical regions of the alignment between enzymes, detailing that the key residues involved in the redox regulation of *Ehi*UDP-Glc PPase are strictly conserved in *Gla*UDP-Glc

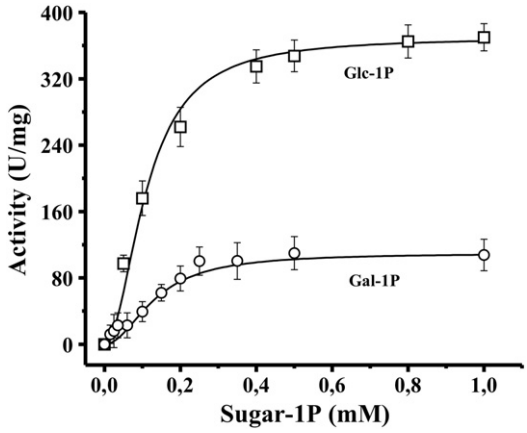

Fig. 2. Saturation plots for Glc-1P (squares) or Gal-1P (circles) of *Gla*UDP-Glc PPase. Activity was measured as detailed under the Materials and methods section. Values are average data of three independent measurements.

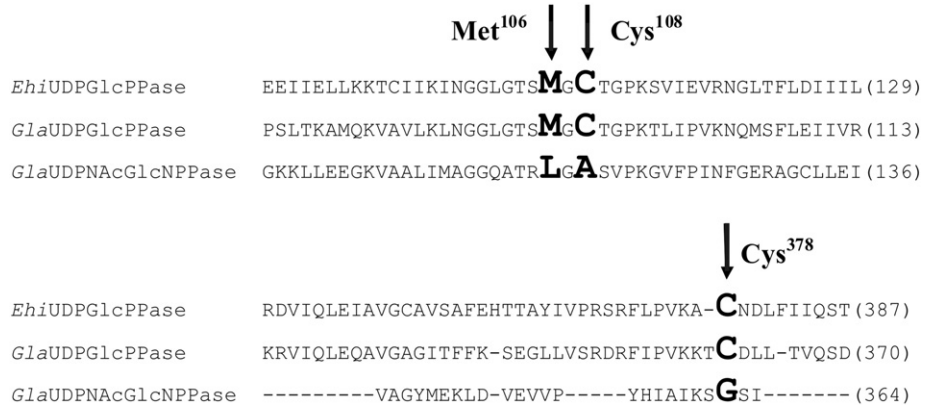

Fig. 3. Alignment between *E. histolytica* UDP-Glc PPase (*Ehi*UDP-GlcPPase), *G. lamblia* UDP-Glc PPase (*Gla*UDP-Glc PPase) and UDP-GlcNAc PPase (*Gla*UDP-GlcNAc PPase). Conserved Cys and Met residues involved in redox regulation (according to [6]) are marked and indicated with arrows.

PPase (Cys^{92}, Cys^{362} and Met^{90}, respectively). On the other hand, the *in silico* analysis in Fig. 3 also shows that *Gla*UDP-GlcNAc PPase (sharing only 13% identity with *Ehi*UDP-Glc PPase) lacks these residues. *Gla*UDP-GlcNAc PPase has eight Cys residues albeit they are not conserved in the other two pyrophosphorylases (see details in Supplemental Fig. 2).

Based on these analyses and to evaluate the effect of redox compounds on the activity of the enzymes under study, we incubated *Gla*UDP-Glc PPase and *Gla*UDP-GlcNAc PPase with H_2O_2 or SNP (0.5 mM and 2 mM each). The former enzyme was inactivated by both oxidants in a time dependent manner (Fig. 4) with a slightly stronger effect of H_2O_2 in comparison to SNP; and both reagents modified *Gla*UDP-Glc PPase to produce a complete loss of the activity after 30 min. The oxidation of *Gla*UDP-Glc PPase produced no change in its oligomeric structure, since fully active (reduced) and inactive (oxidized) enzyme eluted as a single peak of molecular mass 50 kDa when were analyzed by size exclusion chromatography. As shown in Fig. 4, *Gla*UDP-GlcNAc PPase was practically insensitive to both oxidants when incubated under similar conditions. The inactivation of this enzyme required a substantially higher concentration (10 mM) of H_2O_2 or SNP to decrease its activity by 60% or 40%, respectively (data not shown).

Given that the pair Cys/CySS could work as redox buffer in *Giardia* [43] and considering the marked difference in sensitivity to oxidant reagents exhibited by *Gla*UDP-Glc PPase and *Gla*UDP-GlcNAc PPase, we conducted a redox titration related with catalytic capacity. The activity of each enzyme was determined at different redox potentials (E_h) reached by specific ratios of Cys to CySS into the assay media. As depicted in Fig. 5, the activity of *Gla*UDP-Glc PPase decreased as the E_h became more oxidizing, being the enzyme almost completely inactive at −64 mV, with an E_m (potential where it is reached a 50% of activity) calculated at −84 mV. As expected, the enzyme showed the same redox sensitiveness when assayed for activity with Gal-1P. In good agreement with the above results, it was observed a partial loss of *Gla*UDP-GlcNAc PPase activity at higher oxidizing potentials, and the enzyme reached a maximal inhibition of 75% at positive E_h values (Fig. 5).

As has been described [6], redox modulation of *Ehi*UDP-Glc PPase involves not only the inactivation of the enzyme by oxidation but also the recovery of its activity by reducing agents. In our hands a similar behavior was exhibited by *Gla*UDP-Glc PPase; since different chemical and biological agents such as DTT, L-Cys, thioredoxin (*Tcr*TRX) and tryparedoxin (*Tcr*TXN) from *T. cruzi* were effective to rescue the enzyme from its inactive oxidized state. As shown in Fig. 6, the enzyme from *G. lamblia* that has been inactivated by more than 90% by H_2O_2 (similar results were obtained when SNP was the oxidant) was completely reactivated by treatments with DTT, L-Cys or *Tcr*TXN; whilst *Tcr*TRX only partially recovered the enzyme activity to a maximum of ~70% of the original value. Thus, results support the regulation of the synthesis of UDP-Glc by a posttranslational redox mechanism in *G. lamblia*, adding

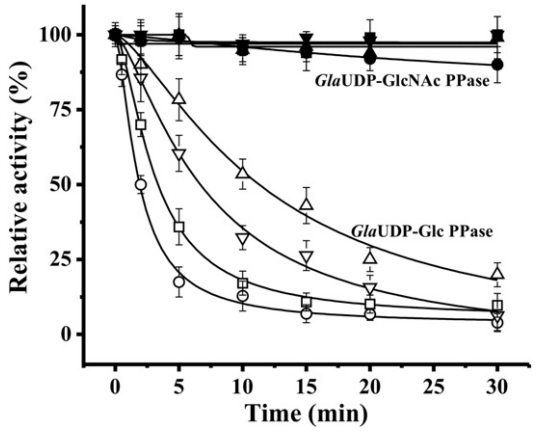

Fig. 4. Oxidation of *Gla*UDP-Glc PPase (open symbols) or *Gla*UDP-GlcNAc PPase (filled symbols). Each enzyme was oxidized with 0.5 (squares) and 2 (circles) mM of H_2O_2 or 0.5 (up triangles) and 2 (down triangles) mM of SNP. At the beginning of oxidation assays both enzymes were fully active (100%) with values of 400 U/mg and 75 U/mg for *Gla*UDP-Glc PPase and *Gla*UDP-GlcNAc PPase, respectively. Results are means of three independent assays.

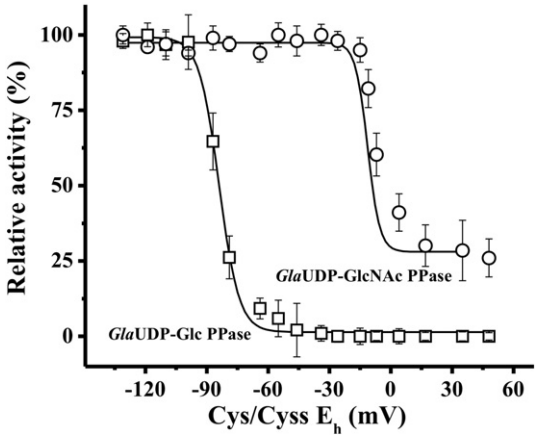

Fig. 5. Activity of *Gla*UDP-Glc PPase and *Gla*UDP-GlcNAc PPase determined at different redox states. Each enzyme was incubated at varying E_h potentials established by different Cys/CySS ratios (Cys/CySS E_h) until redox equilibrium. Then, the respective activity in the direction of UDP-sugar synthesis was assayed. Relative activity for *Gla*UDP-GlcPPase (squares) was measured using 1 mM UTP and 1 mM Glc-1P as substrates; while for *Gla*UDP-GlcNAc PPase (circles) 1 mM UTP and 1.5 mM GlcNAc-1P was employed. One hundred percent of activity corresponds to 400 U/mg (*Gla*UDP-GlcPPase), or 75 U/mg (*Gla*UDP-GlcNAc PPase).

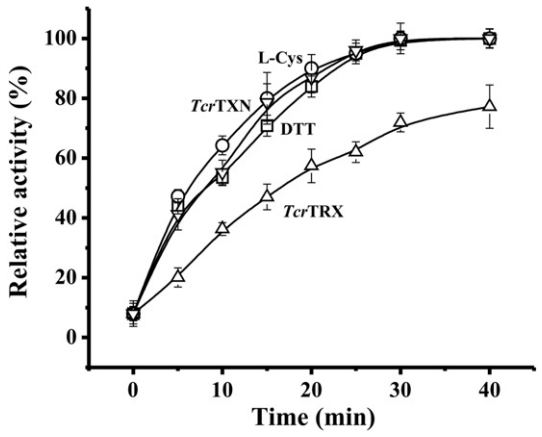

Fig. 6. Effect of reducing agents on inactivated *Gla*UDP-Glc PPase. The enzyme was oxidized for 30 min with 0.5 mM H_2O_2 and then treated during the specified times with 2.5 mM DTT (squares), 5 mM L-Cys (circles), 50 μM reduced *Tcr*TRX (up triangles) or 50 μM reduced *Tcr*TXN (down triangles).

a new example to what could be a characteristic taking place in protozoa [6].

4. Discussion

In the present study, a functionally active UDP-GlcPPase from *G. lamblia* has been biochemically characterized. We cloned the only nucleotide sequence encoding a UTP-glucose-1-phosphate uridylyltransferase (*ugp*), reported in the *G. lamblia* database, and followed with its heterologous expression in *E. coli*. The purified recombinant enzyme presented a monomeric structure and it exhibited distinctive characteristics, mainly for the ability to use TTP and Gal-1P as substrates, besides the use of UTP and Glc-1P. Oxidation by physiological compounds (hydrogen peroxide and nitric oxide generated by SNP) inactivated the enzyme and the process was reverted after reduction by cysteine and thioredoxin. Results are of relevance in the framework of the role played by NDP-sugars (in general) and by UDP-Glc/UDP-Gal (in particular) for the *Giardia* physiology and considering the scarce information currently available on the subject.

In parasitic organisms, the formation of NDP-sugars followed by their use by specific glycosyl transferases are critical processes, since synthesis of certain structural oligo and polysaccharides determines the capacity of interaction with other cells [44]. Therefore, glycosidic compounds in these organisms play an important role in attachment and invasion to host cells and also for induction and modulation of the host immune response [45]. Besides, the involvement of UDP-Glc and UDP-Gal as key metabolites in *G. lamblia* is supported by: (i) the parasite ability to accumulate glycogen (for storage of carbon and energy, which determine survival and pathogenic capacity) [11,12]; and (ii) Gal represents a 14 and 26% of total sugars present in glycosidic structures of trophozoites and cyst membranes, respectively [45].

The Leloir pathway is considered as a route connecting Gal and Glc in 3 steps: phosphorylation of Gal by galactokinase (EC: 2.7.1.6), then activation of Gal-1P into UDP-Gal mediated by UDP-glucose:α-D-galactose-1-phosphate uridylyltransferase (GalT; EC 2.7.7.12), and a last reaction involving epimerization of the sugar at C4 by UDP-Glc 4-epimerase (EC-5.3.1.2) [46] (Fig. 7A). GalT is absent in most of protozoa, but (interestingly) alternative pathways for UDP-Gal synthesis exist [47–49] (Fig. 7A). For example, in *L. major* a UDP-sugar PPase (EC: 2.7.7.64) with broad specificity toward sugar-1P has been reported [47]; the enzyme preferentially activates Glc-1P and Gal-1P to UDP-Glc and UDP-Gal, respectively, with a 2.4-fold higher catalytic efficiency for the latter substrate. Similarly, a UDP-sugar PPase from *T. cruzi* uses Gal-1P and Glc-1P as principal substrates, exhibiting a catalytic efficiency 3.8-fold lower toward Gal-1P in comparison to Glc-1P [49].

An in silico analysis of the genome from *G. lamblia* shows that genes encoding galactokinase and GalT are absent. Instead, a gene coding for UDP-Glc epimerase, a putative protein that shares 26% of identity with the homologous enzyme from *T. cruzi*, is found. In addition, *G. lamblia* lacks a gene encoding an UDP-sugar PPase and it only presents two genes linked to UTP-dependent pyrophosphorylases: those that encode the UDP-Glc PPase and the UDP-GlcNAc PPase. The latter enzyme has been extensively characterized; its behavior concerning kinetic

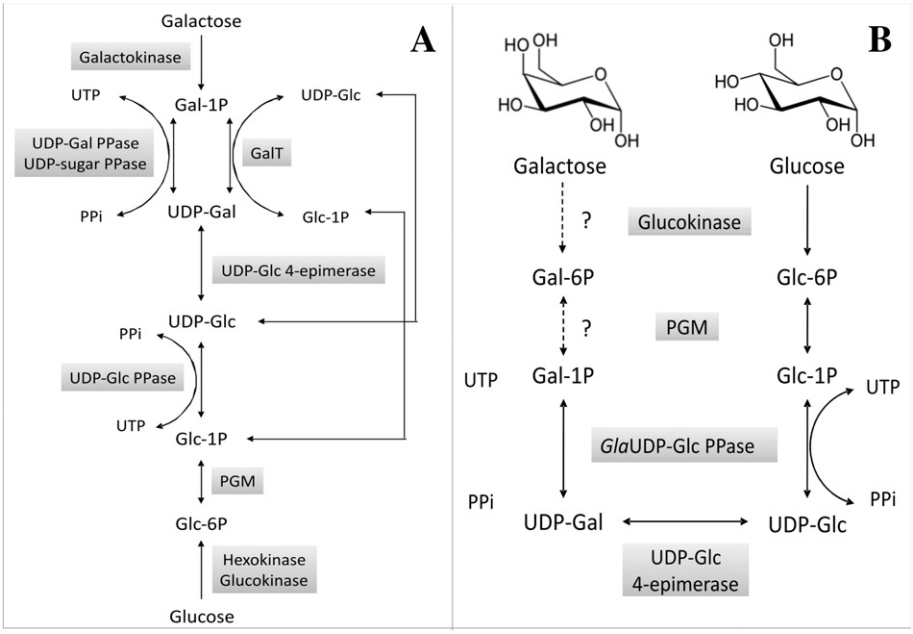

Fig. 7. Metabolic pathways for UDP-Glc and UDP-Gal. (A) Alternative metabolism for the synthesis of Gal. The Leloir pathway connects Gal and Glc involving the steps catalyzed by galactokinase, GalT and UDP-Glc 4-epimerase. An alternative pathway for UDP-Gal synthesis is the activation of Gal-1P into UDP-Gal by UDP-Gal PPase [48] or by UDP-sugar PPase. (B) Scheme proposed for the metabolism taking place in *G. lamblia*. The scheme is based on the absence of GalT, UDP-Gal PPase and UDP-sugar PPase, as well as on the properties herein determined for *Gla*UDP-Glc PPase related with its ability to catalyze synthesis of UDP-Gal from Gal-1P and UTP. The proposed metabolism involves two steps to convert Gal into Gal-1P mediated by glucokinase [50] and PGM [51], which could exhibit some degree of promiscuity.

parameters and high specificity toward GlcNAc-1P gave results that are in good agreement with previous reports [15,34]. Conversely, *Gla*UDP-Glc PPase showed ability to use Gal-1P as an alternative substrate to synthesize UDP-Gal with apparent affinity and catalytic efficiency practically similar to the production of UDP-Glc from Glc-1P and UTP.

In this scenario, functional roles for synthesis of UDP-Glc/UDP-Gal and salvage of monosaccharide could be ascribed to the unique *Gla*UDP-Glc PPase that was characterized herein (Fig. 7B); while UDP-GlcNAc PPase would be involved in the metabolism of UDP-GlcNAc (and perhaps other UDP-sugarNAc) [34]. The possible metabolism of Gal in *G. lamblia* via the reaction catalyzed by *Gla*UDP-Glc PPase has as a major problem the absence of galactokinase in the parasite. Previous works reported that glucokinase (EC 2.7.1.2) [50] and phosphoglucomutase (PGM; EC 5.4.2.2) [51] present in this organism exhibit deeply distinctive functional properties. Also, it is worth to consider that *Giardia* is an early diverging eukaryote with many unusual features of ultrastructure, metabolism and gene sequence [7]. Thus, it is tempting to speculate that the odd characteristics of these enzymes also include some degree of promiscuity toward sugars (not yet proven for Gal), thus setting up a two steps path to convert Gal into Gal-1P (Fig. 7B).

Synthesis of UDP-sugars in *Giardia* seems to present singular differences regarding other protozoa. For example, *G. lamblia* lacks a broad spectrum UDP-sugar PPase, such as was found in *Trypanosoma* and *Leishmania* [47,49]. The occurrence of a unique *Gla*UDP-Glc PPase producing UDP-Glc and UDP-Gal also appears different to the characteristics of homologous enzymes in *E. histolytica*. We found that the amoebian UDP-Glc PPase recently characterized [6] exhibits less than 1% of activity with Gal-1P and it is highly specific towards Glc-1P. These results are in good agreement with previous work [48] reporting that an enzyme with activity of UDP-Gal PPase (EC 2.7.7.10) could be separated from UDP-Glc PPase in extracts obtained from the microorganism. On the other hand, mammalian UDP-Glc PPases can use UDP-Gal, but with significantly lower capacity when compared to UDP-Glc [52]. This occurs even in barley, since it has been recently reported that the UDP-Glc PPase from this source is able to catalyze Gal-1P consumption but with a very low efficiency compared to Glc-1P [42].

The use of TTP by UDP-Glc PPase has been reported for the enzyme from some bacteria [1,4,53,54], which is structurally different from that of eukaryotes, sharing no more that 8% identity at the amino acid level between them [2,55]. The results regarding the capacity of *Gla*UDP-Glc PPase for the use of TTP as an alternative substrate to UTP also constitute a singular behavior, since homologous enzymes from plants, fungi and particularly protozoan were reported highly specific for UTP [6,36,37,39]. An exception was stated with a mammalian UDP-Glc PPase that catalyzes the pyrophosphorolysis of TDP-Glc but with low efficiency [52]. As a whole, the comparison regarding substrate specificity exhibited by *Gla*UDP-Glc PPase and *Gla*UDP-GlcNAc PPase suggests that the former would be the only enzyme mainly involved in synthesis of UDP-Glc and UDP-Gal in *Giardia*.

G. lamblia UDP-Glc PPase presents clear homology with eukaryotic UDP-Glc PPase (~30–40% identity, as mentioned above), and a lower identity to UDP-sugar and UDP-GlcNAc PPases (lower than 15%). Analysis of these pyrophosphorylases showed that the enzymes had maintained a conserved fold throughout evolution [49]. In particular, the glycine-rich consensus motif essential for the catalysis is highly conserved and additional residues involved in the uridine and phosphate binding [47,49]. However, residues interacting with the glucose moiety in UDP-Glc PPases are not conserved in UDP-sugar PPase, and it is likely that insertion of loops between the conserved structural domains generated many changes during evolution to allow the specific enzyme to be either strict to the substrate or to accept different substrates [47,49].

To explore for possible relationships between protein structure and the ability to use of alternative substrates by *Gla*UDP-Glc PPase, we made an amino acids alignment with other UDP-Glc PPases, highly specific for UTP and Glc-1P. Supplemental Fig. 3 pinpoints the nucleotide-binding loop (region K80–K95), the sugar-binding loop (region R249–R261), and the residues identified as critical for binding of substrates to the *L. major* enzyme (which crystal structure has been solved [3,56]): for Glc-1P residues Asn^{219}, Glu^{284}, Asn^{306}, Thr^{307}, Asn^{308}, and Phe^{376}; and for UTP-binding residues Met^{130}, Gln^{162}, Gly^{190}, His^{191}, Asn^{219}, Asp^{221}. It is shown that all these residues are strictly conserved in the alignment, except for Asn^{219} and Thr^{307} that only in *Gla*UDP-Glc PPase are different and replaced by Ser and Val, respectively.

In addition, UDP-Glc PPases found in fungi and animals are active as octamers [37,38] but the enzymes from plants and protozoa were observed in an active monomeric form [6,35,36,39,57]. In this work, we showed that *Gla*UDP-Glc PPase is active as a monomer, as also is the case for *Gla*UDP-GlcNAc PPase. Although it has been demonstrated that the enzyme from barley can adopt different oligomeric structures strongly affecting its catalytic capacity [57], no other conformation (besides the monomer) was detected for the *G. lamblia* enzyme, even in its oxidized state. This agrees with results described for the enzyme from *E. hystolitica* [6] and *L. major* [36], which support that regulation of UDP-Glc PPase activity in protozoan organisms by oligomeric sequestration would not be as relevant as in plants [57].

It is worth to note that in spite of its monomeric structure *Gla*UGP-Glc PPase showed positive cooperativity for the use of substrates (especially for alternative ones). Traditionally, cooperativity is viewed as requiring the participation of multiple, spatially distinct binding sites related with oligomeric proteins. Albeit, it has been reported a few examples of monomeric enzymes exhibiting cooperative effects [23,24], and there has been described different models that could explain this non-Michaelis–Menten kinetic behavior [26]. An extensively studied example is mammalian glucokinase [58]. This enzyme is able to use different sugars and phosphoryl donors as substrates depicting distinctive kinetic behavior. Glucokinase displays a sigmoidal saturation curve for glucose, but it was observed that cooperativity is lost when it uses a poor nucleotide substrate (ITP) as phosphoryl donor. Furthermore, when the enzyme uses the analogue substrate 2-deoxyglucose the saturation curve becomes hyperbolic [58]. Several models for the kinetic behavior of glucokinase have been proposed [59,60]. The elucidation of the protein structure [59] allowed to propose a mechanism explaining the positive cooperativity exhibited by this monomeric enzyme with one substrate and not with the other. In addition, different studies demonstrated that the distinctive kinetic behavior with alternative substrates would be the consequence of differences in the velocities of the conformational transitions induced by them [58,60,61]. Thus, the model proposed for glucokinase seems a good example to explain the occurrence of cooperativity in the kinetics for the use of Gal-1P and TTP by monomeric *Gla*UDP-Glc PPase.

Regarding regulation of UDP-Glc PPases, different posttranscriptional [62] and posttranslational [2,6,63,64] modifications have been reported. In particular, we focus this study on the redox mechanism of regulation. It is widely known that a major posttranslational regulation mechanism involves inactivation/activation of this enzyme via oxidation–reduction reactions [28,29]. Certainly, the *E. hystolytica* UDP-Glc PPase was the first reported to be subjected to redox regulation in protozoa [6] and in the current study we further explored this issue on both enzymes involved in UDP-sugar metabolism in *G. lamblia*. Results showed that the redox modulation of the *Gla*UDP-GlcPPase activity seems to be mediated by a mechanism involving oxidative and reductive agents normally found in vivo. The enzyme is sensitive to oxidative inactivation by physiological redox compounds (H_2O_2, SNP), as well as to low molecular weight metabolites and redox proteins (L-Cys, *Tcr*TRX) that can reduce the oxidized enzyme with complete recovery of its activity. Such a redox regulation of the activity was not observed for *Gla*UDP-GlcNAc PPase. This enzyme was less sensitive to redox changes, since besides the high oxidizing conditions required to reduce its activity, the following incubation with different reducing agents was ineffective to revert the process (data not shown).

It is known that hydrogen peroxide and nitric oxide act as key redox metabolites involved in different intracellular signaling under physiological and stress conditions [65–67]. Parasitic protozoa not only have to eliminate their endogenous toxic metabolites but they must also cope with the oxidative response of the host immune system [43]. Therefore, antioxidant and detoxification systems, such as L-Cys and TRX, play critical role in degradation of reactive oxygen species and they participate in mechanisms for regulating the activity of enzymes through posttranslational modification [43,68]. Thus, in *G. lamblia* (as in *E. hystolytica* [6] and probably other protozoa) these oxidant/reducing cell mediators could be involved in modifying specific proteins, being UDP-GlcPPase one of the targets.

In addition, redox titration experiments determined that the activity of *Gla*UDP-Glc PPase decreased as the E_h turned to oxidizing conditions, with a complete inhibition at −60 mV. This E_h value and the presence of a Cys/CySS redox buffer is functional in the organism [43], thus giving support to the physiological significance of the redox regulation of UDP-sugar synthesis in *G. lamblia*. In contrast, under this condition *Gla*UDP-GlcNAc PPase remained fully active, as the enzyme required higher E_h values (out of the expected physiological range) to become inhibited in its catalytic capacity. It is known that *G. lamblia* is a microaerophilic parasite having a limited capacity to detoxify O_2 and its reactive species [69] and differing from other eukaryotes in that it lacks of glutathione as a redox buffer. Nevertheless, it has been speculated that Cys itself could act as the key antioxidant and/or redox buffer [43], and a thioredoxin reductase using Cys as primary electron acceptor has been identified in the microorganism [70].

As a whole, our results suggest that *G. lamblia* could efficiently manage the pool of hexose-1P to produce diverse sugar-nucleotides that serve for synthesis of different saccharides (glycogen as well structural oligo and polysaccharides) determining survival and pathogenesis of the parasite. The properties of *Gla*UDP-Glc PPase characterized in the present work strongly support that the metabolism of carbohydrates utilizing UDP-Glc and UDP-Gal could be strictly controlled with a dependence on the levels of redox metabolites in the intracellular environment. Also, the sensitivity to redox agents found for *Gla*UDP-Glc PPase (similar to that reported for the enzyme from *E. histolytica* [6]) constitute a new example on the possible occurrence of a redox mechanism to regulate carbohydrate metabolism in protozoa. On the other hand, the capacity of the enzyme to use Gal-1P and produce UDP-Gal opens the view that the monosaccharide would be particularly metabolized in *G. lamblia*. Further studies are necessary to establish the complete picture of such a specific metabolism, mainly to determine which enzymes are specifically involved in the conversion of Gal into Gal-1P. The better understanding of the metabolism of Gal in *G. lamblia* is critical, because of the involvement of the sugar as a main component of certain cellular structures that are vital for the parasite physiology.

Acknowledgements

This work was supported by Agencia Nacional de Promoción Científica y Tecnológica (PICT'11-1986 and PICT'12-2439); Consejo Nacional de Investigaciones Científicas y Técnicas (PIP 112-201101-00438); and Universidad Nacional del Litoral (CAI+D 2011 & Orientados).

Appendix A. Supplementary data

Supplementary data to this article can be found online at http://dx.doi.org/10.1016/j.bbagen.2014.10.002.

References

[1] M.B. Bosco, M. Machtey, A.A. Iglesias, M. Aleanzi, UDPglucose pyrophosphorylase from *Xanthomonas* spp. Characterization of the enzyme kinetics, structure and inactivation related to oligomeric dissociation, Biochimie 91 (2009) 204–213.
[2] L.A. Kleczkowski, M. Geisler, I. Ciereszko, H. Johansson, UDP-glucose pyrophosphorylase. An old protein with new tricks, Plant Physiol. 134 (2004) 912–918.
[3] T. Steiner, A.C. Lamerz, P. Hess, C. Breithaupt, S. Krapp, G. Bourenkov, R. Huber, R. Gerardy-Schahn, U. Jacob, Open and closed structures of the UDP-glucose pyrophosphorylase from *Leishmania major*, J. Biol. Chem. 282 (2007) 13003–13010.
[4] M.D. Asencion Diez, A.C. Ebrecht, L.I. Martinez, M.C. Aleanzi, S.A. Guerrero, M.A. Ballicora, A.A. Iglesias, A chimeric UDP-glucose pyrophosphorylase produced by protein engineering exhibits sensitivity to allosteric regulators, Int. J. Mol. Sci. 14 (2013) 9703–9721.
[5] J.B. Thoden, H.M. Holden, The molecular architecture of glucose-1-phosphate uridylyltransferase, Protein Sci. 16 (2007) 432–440.
[6] L.I. Martinez, C.V. Piattoni, S.A. Garay, D.E. Rodrigues, S.A. Guerrero, A.A. Iglesias, Redox regulation of UDP-glucose pyrophosphorylase from *Entamoeba histolytica*, Biochimie 93 (2011) 260–268.
[7] D. Lloyd, J.C. Harris, *Giardia*: highly evolved parasite or early branching eukaryote? Trends Microbiol. 10 (2002) 122–127.
[8] H.G. Morrison, A.G. McArthur, F.D. Gillin, S.B. Aley, R.D. Adam, G.J. Olsen, A.A. Best, W.Z. Cande, F. Chen, M.J. Cipriano, B.J. Davids, S.C. Dawson, H.G. Elmendorf, A.B. Hehl, M.E. Holder, S.M. Huse, U.U. Kim, E. Lasek-Nesselquist, G. Manning, A. Nigam, J.E. Nixon, D. Palm, N.E. Passamaneck, A. Prabhu, C.I. Reich, D.S. Reiner, J. Samuelson, S.G. Svard, M.L. Sogin, Genomic minimalism in the early diverging intestinal parasite *Giardia lamblia*, Science 317 (2007) 1921–1926.
[9] A.B. Lopez, K. Sener, E.L. Jarroll, H. van Keulen, Transcription regulation is demonstrated for five key enzymes in *Giardia intestinalis* cyst wall polysaccharide biosynthesis, Mol. Biochem. Parasitol. 128 (2003) 51–57.
[10] H.D. Lujan, M.R. Mowatt, T.E. Nash, Mechanisms of *Giardia lamblia* differentiation into cysts, Microbiol. Mol. Biol. Rev. 61 (1997) 294–304.
[11] R.B. Ladeira, M.A. Freitas, E.F. Silva, N.F. Gontijo, M.A. Gomes, Glycogen as a carbohydrate energy reserve in trophozoites of *Giardia lamblia*, Parasitol. Res. 96 (2005) 418–421.
[12] P. Pradhan, S.W. Lundgren, W.A. Wilson, A. Brittingham, Glycogen storage and degradation during in vitro growth and differentiation of *Giardia intestinalis*, J. Parasitol. 98 (2012) 442–444.
[13] D.A. Bulik, D.G. Lindmark, E.L. Jarroll, Purification and characterization of UDP-N-acetylglucosamine pyrophosphorylase from encysting *Giardia*, Mol. Biochem. Parasitol. 95 (1998) 135–139.
[14] M.T. Mok, M.R. Edwards, Critical sources of error in colorimetric assay for UDP-N-acetylglucosamine pyrophosphorylase, Anal. Biochem. 343 (2005) 341–343.
[15] M.T. Mok, E. Tay, E. Sekyere, W.K. Glenn, A.S. Bagnara, M.R. Edwards, *Giardia intestinalis*: molecular characterization of UDP-N-acetylglucosamine pyrophosphorylase, Gene 357 (2005) 73–82.
[16] M.A. Ballicora, A.A. Iglesias, J. Preiss, ADP-glucose pyrophosphorylase, a regulatory enzyme for bacterial glycogen synthesis, Microbiol. Mol. Biol. Rev. 67 (2003) 213–225.
[17] M.A. Ballicora, A.A. Iglesias, J. Preiss, ADP-Glucose pyrophosphorylase: a regulatory enzyme for plant starch synthesis, Photosynth. Res. 79 (2004) 1–24.
[18] J. Sambrook, D.W. Russell, Molecular Cloning: A Laboratory Manual, Third edition Cold Spring Harbor Laboratory Press, Cold Spring Harbor, New York, 2001.
[19] M. Bradford, A rapid and sensitive method for the quantitation of microgram quantities of protein utilizing the principle of protein-dye binding, Anal. Biochem. 72 (1976) 248–254.
[20] U.K. Laemmli, Cleavage of structural proteins during the assembly of the head of bacteriophage T4, Nature 227 (1970) 680–685.
[21] C. Fusari, A.M. Demonte, C.M. Figueroa, M. Aleanzi, A.A. Iglesias, A colorimetric method for the assay of ADP-glucose pyrophosphorylase, Anal. Biochem. 352 (2006) 145–147.
[22] M. Dixon, E.C. Webb, Enzyme Techniques, Enzymes, Academic Press, New York, 1979.
[23] L.R. Vicario, D.F. Gómez Casati, A.A. Iglesias, A simple laboratory experiment for the teaching of the assay and kinetic characterization of enzymes, Biochem. Educ. 25 (1997) 106–109.
[24] M.A. Ballicora, E.D. Erben, T. Yazaki, A.L. Bertolo, A.M. Demonte, J.R. Schmidt, M. Aleanzi, C.M. Bejar, C.M. Figueroa, C.M. Fusari, A.A. Iglesias, J. Preiss, Identification of regions critically affecting kinetics and allosteric regulation of the *Escherichia coli* ADP-glucose pyrophosphorylase by modeling and pentapeptide-scanning mutagenesis, J. Bacteriol. 189 (2007) 5325–5333.
[25] A. Cornish-Bowden, M.L. Cardenas, Specificity of non-Michaelis–Menten enzymes: necessary information for analyzing metabolic pathways, J. Phys. Chem. B 114 (2010) 16209–16213.
[26] C.M. Porter, B.G. Miller, Cooperativity in monomeric enzymes with single ligand-binding sites, Bioorg. Chem. 43 (2012) 44–50.
[27] S. Aleryani, E. Milo, P. Kostka, Formation of peroxynitrite during thiol-mediated reduction of sodium nitroprusside, Biochim. Biophys. Acta 1472 (1999) 181–190.
[28] C.V. Piattoni, S.A. Guerrero, A.A. Iglesias, A differential redox regulation of the pathways metabolizing glyceraldehyde-3-phosphate tunes the production of reducing power in the cytosol of plant cells, Int. J. Mol. Sci. 14 (2013) 8073–8092.
[29] C.V. Piattoni, V.S. Blancato, H. Miglietta, A.A. Iglesias, S.A. Guerrero, On the occurrence of thioredoxin in *Trypanosoma cruzi*, Acta Trop. 97 (2006) 151–160.
[30] F.Q. Schafer, G.R. Buettner, Redox environment of the cell as viewed through the redox state of the glutathione disulfide/glutathione couple, Free Radic. Biol. Med. 30 (2001) 1191–1212.
[31] J.W. Zhu, J.F. Yuan, H.M. Yang, S.T. Wang, C.G. Zhang, L.L. Sun, H. Yang, H. Zhang, Extracellular cysteine (Cys)/cystine (CySS) redox regulates metabotropic glutamate receptor 5 activity, Biochimie 94 (2012) 617–627.
[32] N. Rouhier, E. Gelhaye, J.M. Gualberto, M.N. Jordy, E. De Fay, M. Hirasawa, S. Duplessis, S.D. Lemaire, P. Frey, F. Martin, W. Manieri, D.B. Knaff, J.P. Jacquot, Poplar

peroxiredoxin Q. A thioredoxin-linked chloroplast antioxidant functional in pathogen defense, Plant Physiol. 134 (2004) 1027–1038.
[33] C. Aurrecoechea, J. Brestelli, B.P. Brunk, J.M. Carlton, J. Dommer, S. Fischer, B. Gajria, X. Gao, A. Gingle, G. Grant, O.S. Harb, M. Heiges, F. Innamorato, J. Iodice, J.C. Kissinger, E. Kraemer, W. Li, J.A. Miller, H.G. Morrison, V. Nayak, C. Pennington, D.F. Pinney, D.S. Roos, C. Ross, C.J. Stoeckert Jr., S. Sullivan, C. Treatman, H. Wang, GiardiaDB and TrichDB: integrated genomic resources for the eukaryotic protist pathogens *Giardia lamblia* and *Trichomonas vaginalis*, Nucleic Acids Res. 37 (2009) D526–D530.
[34] M.T. Mok, M.R. Edwards, Kinetic and physical characterization of the inducible UDP-N-acetylglucosamine pyrophosphorylase from *Giardia intestinalis*, J. Biol. Chem. 280 (2005) 39363–39372.
[35] K. Marino, M.L. Guther, A.K. Wernimont, M. Amani, R. Hui, M.A. Ferguson, Identification, subcellular localization, biochemical properties, and high-resolution crystal structure of *Trypanosoma brucei* UDP-glucose pyrophosphorylase, Glycobiology 20 (2010) 1619–1630.
[36] A.C. Lamerz, T. Haselhorst, A.K. Bergfeld, M. von Itzstein, R. Gerardy-Schahn, Molecular cloning of the *Leishmania major* UDP-glucose pyrophosphorylase, functional characterization, and ligand binding analyses using NMR spectroscopy, J. Biol. Chem. 281 (2006) 16314–16322.
[37] A. Roeben, J.M. Plitzko, R. Korner, U.M. Bottcher, K. Siegers, M. Hayer-Hartl, A. Bracher, Structural basis for subunit assembly in UDP-glucose pyrophosphorylase from *Saccharomyces cerevisiae*, J. Mol. Biol. 364 (2006) 551–560.
[38] Y. Konishi, K. Tanizawa, S. Muroya, T. Fukui, Molecular cloning, nucleotide sequencing, and affinity labeling of bovine liver UDP-glucose pyrophosphorylase, J. Biochem. 114 (1993) 61–68.
[39] F. Martz, M. Wilczynska, L.A. Kleczkowski, Oligomerization status, with the monomer as active species, defines catalytic efficiency of UDP-glucose pyrophosphorylase, Biochem. J. 367 (2002) 295–300.
[40] S.K. Gupta, J.R. Sowokinos, I.S. Hahn, Regulation of UDP-glucose pyrophosphorylase isozyme UGP5 associated with cold-sweetening resistance in potatoes, J. Plant Physiol. 165 (2008) 679–690.
[41] M. Meng, M. Wilczynska, L.A. Kleczkowski, Molecular and kinetic characterization of two UDP-glucose pyrophosphorylases, products of distinct genes, from *Arabidopsis*, Biochim. Biophys. Acta 1784 (2008) 967–972.
[42] D. Decker, M. Meng, A. Gornicka, A. Hofer, M. Wilczynska, L.A. Kleczkowski, Substrate kinetics and substrate effects on the quaternary structure of barley UDP-glucose pyrophosphorylase, Phytochemistry 79 (2012) 39–45.
[43] S. Muller, E. Liebau, R.D. Walter, R.L. Krauth-Siegel, Thiol-based redox metabolism of protozoan parasites, Trends Parasitol. 19 (2003) 320–328.
[44] A. Dickmanns, S. Damerow, P. Neumann, E.C. Schulz, A.C. Lamerz, F.H. Routier, R. Ficner, Structural basis for the broad substrate range of the UDP-sugar pyrophosphorylase from *Leishmania major*, J. Mol. Biol. 405 (2011) 461–478.
[45] E. Ortega-Barria, H.D. Ward, J.E. Evans, M.E. Pereira, N-acetyl-D-glucosamine is present in cysts and trophozoites of *Giardia lamblia* and serves as receptor for wheatgerm agglutinin, Mol. Biochem. Parasitol. 43 (1990) 151–165.
[46] P.A. Frey, The Leloir pathway: a mechanistic imperative for three enzymes to change the stereochemical configuration of a single carbon in galactose, FASEB J. 10 (1996) 461–470.
[47] S. Damerow, A.C. Lamerz, T. Haselhorst, J. Fuhring, P. Zarnovican, M. von Itzstein, F.H. Routier, *Leishmania* UDP-sugar pyrophosphorylase: the missing link in galactose salvage? J. Biol. Chem. 285 (2010) 878–887.
[48] P.A. Lobelle-Rich, R.E. Reeves, Separation and characterization of two UTP-utilizing hexose phosphate uridylyltransferases from *Entamoeba histolytica*, Mol. Biochem. Parasitol. 7 (1983) 173–182.
[49] T. Yang, M. Bar-Peled, Identification of a novel UDP-sugar pyrophosphorylase with a broad substrate specificity in *Trypanosoma cruzi*, Biochem. J. 429 (2010) 533–543.
[50] K. Henze, D.S. Horner, S. Suguri, D.V. Moore, L.B. Sanchez, M. Muller, T.M. Embley, Unique phylogenetic relationships of glucokinase and glucosephosphate isomerase of the amitochondriate eukaryotes *Giardia intestinalis*, *Spironucleus barkhanus and Trichomonas vaginalis*, Gene 281 (2001) 123–131.
[51] S. Mitra, J. Cui, P.W. Robbins, J. Samuelson, A deeply divergent phosphoglucomutase (PGM) of *Giardia lamblia* has both PGM and phosphomannomutase activities, Glycobiology 20 (2010) 1233–1240.
[52] R.L. Turnquist, T.A. Gillett, R.G. Hansen, Uridine diphosphate glucose pyrophosphorylase. Crystallization and properties of the enzyme from rabbit liver and species comparisons, J. Biol. Chem. 249 (1974) 7695–7700.
[53] M.D. Asencion Diez, S. Peiru, A.M. Demonte, H. Gramajo, A.A. Iglesias, Characterization of recombinant UDP- and ADP-glucose pyrophosphorylases and glycogen synthase to elucidate glucose-1-phosphate partitioning into oligo- and polysaccharides in *Streptomyces coelicolor*, J. Bacteriol. 194 (2012) 1485–1493.
[54] A.C. Weissborn, Q. Liu, M.K. Rumley, E.P. Kennedy, UTP: alpha-D-glucose-1-phosphate uridylyltransferase of *Escherichia coli*: isolation and DNA sequence of the galU gene and purification of the enzyme, J. Bacteriol. 176 (1994) 2611–2618.
[55] L.A. Kleczkowski, M. Geisler, E. Fitzek, M. Wilczynska, A common structural blueprint for plant UDP-sugar-producing pyrophosphorylases, Biochem. J. 439 (2011) 375–379.
[56] J. Führing, J.T. Cramer, F.H. Routier, A.C. Lamerz, P. Baruch, R. Gerardy-Schahn, R. Fedorov, Catalytic mechanism and allosteric regulation of UDP-glucose pyrophosphorylase from *Leishmania major*, ACS Catal. 3 (2013) 9.
[57] L.A. Kleczkowski, F. Martz, M. Wilczynska, Factors affecting oligomerization status of UDP-glucose pyrophosphorylase, Phytochemistry 66 (2005) 2815–2821.
[58] M.A. Moukil, E. Van Schaftingen, Analysis of the cooperativity of human beta-cell glucokinase through the stimulatory effect of glucose on fructose phosphorylation, J. Biol. Chem. 276 (2001) 3872–3878.
[59] K. Kamata, M. Mitsuya, T. Nishimura, J. Eiki, Y. Nagata, Structural basis for allosteric regulation of the monomeric allosteric enzyme human glucokinase, Structure 12 (2004) 429–438.
[60] S.X. Lin, K.E. Neet, Demonstration of a slow conformational change in liver glucokinase by fluorescence spectroscopy, J. Biol. Chem. 265 (1990) 9670–9675.
[61] M.L. Cardenas, E. Rabajille, H. Niemeyer, Suppression of kinetic cooperativity of hexokinase D (glucokinase) by competitive inhibitors. A slow transition model, Eur. J. Biochem. 145 (1984) 163–171.
[62] L.A. Kleczkowski, D. Decker, M. Wilczynska, UDP-sugar pyrophosphorylase: a new old mechanism for sugar activation, Plant Physiol. 156 (2011) 3–10.
[63] J. Rutter, B.L. Probst, S.L. McKnight, Coordinate regulation of sugar flux and translation by PAS kinase, Cell 111 (2002) 17–28.
[64] L. Wells, S.A. Whelan, G.W. Hart, O-GlcNAc: a regulatory post-translational modification, Biochem. Biophys. Res. Commun. 302 (2003) 435–441.
[65] S.G. Rhee, Cell signaling. H2O2, a necessary evil for cell signaling, Science 312 (2006) 1882–1883.
[66] M.W. Foster, D.T. Hess, J.S. Stamler, Protein S-nitrosylation in health and disease: a current perspective, Trends Mol. Med. 15 (2009) 391–404.
[67] D.T. Hess, A. Matsumoto, S.O. Kim, H.E. Marshall, J.S. Stamler, Protein S-nitrosylation: purview and parameters, Nat. Rev. Mol. Cell Biol. 6 (2005) 150–166.
[68] Y. Meyer, B.B. Buchanan, F. Vignols, J.P. Reichheld, Thioredoxins and glutaredoxins: unifying elements in redox biology, Annu. Rev. Genet. 43 (2009) 335–367.
[69] D. Lloyd, J.C. Harris, S. Maroulis, G.A. Biagini, R.B. Wadley, M.P. Turner, M.R. Edwards, The microaerophilic flagellate *Giardia intestinalis*: oxygen and its reaction products collapse membrane potential and cause cytotoxicity, Microbiology 146 (Pt 12) (2000) 3109–3118.
[70] D.M. Brown, J.A. Upcroft, P. Upcroft, A thioredoxin reductase-class of disulphide reductase in the protozoan parasite *Giardia duodenalis*, Mol. Biochem. Parasitol. 83 (1996) 211–220.